BeFORECAST

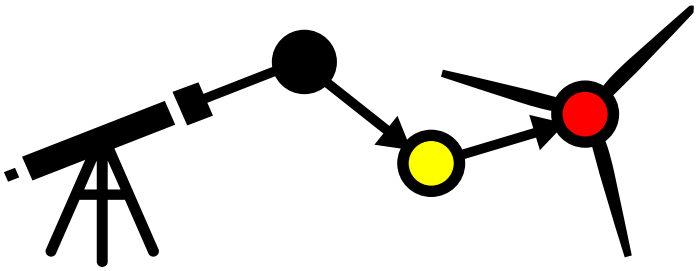

Deliverable: Intercomparison of mesoscale models including wind-farm parameterization implementations

Deliverable No.: D4.2

economie
FOD Economie, K.M.O., Middenstand en Energie

This project has received funding from the Energy Transition Fund of the Belgian Federal Public Service for Economy, SMEs, and Energy (FOD Economie, KMO, Middenstand en Energie)

DOCUMENT CONTROL SHEET

DOCUMENT INFORMATION	
Document title	Intercomparison of mesoscale models including wind-farm parameterization implementations
Author(s), (organization)	Simone Gremmo (VKI), Wim Munters (VKI), Geert Smet (RMI), Dieter Van den Bleeken (RMI)
Deliverable No.	D4.2
Work Package No.	WP4
Lead beneficiary	VKI
Dissemination level	Public
Date of issue	30/11/2025

DOCUMENT SUMMARY

This deliverable presents an intercomparison of mesoscale models and wind farm parameterizations to assess their ability to predict wind speed in offshore wind farms. The study focuses on WRF and ALARO, evaluating configurations with and without wind farm parameterization (WFP). Two parameterizations are considered: the widely used Fitch scheme and the novel Ma & Archer approach, which introduces sub-grid wake modeling. The analysis uses datasets created by VKI and RMI covering different years. Both long-term performance and extreme events, such as Storm Eunice, are examined and assessed through comparisons with lidar measurements inside a Belgian offshore wind farm.

Results show that neglecting wake effects leads to systematic overestimation of wind speed, with bias around +1.25 m/s and mean absolute error (MAE) near 2.0 m/s. Activating WFP reduces bias to approximately -0.25 m/s and lowers MAE to 1.4 m/s, confirming the benefit of wake-aware modeling. Both ALARO and WRF perform similarly when WFP is active, although WRF tends to predict larger wake deficits. Overall, the study demonstrates that incorporating WFP significantly improves forecast accuracy and provides a foundation for further refinement of wake modeling in mesoscale simulations.

Table of Contents

1 Introduction

With more offshore wind farms being installed, it is becoming increasingly important to account for the impact of these farms on regional weather conditions to provide accurate wind and power forecasts. Wind farm operations and power production are negatively affected by wakes originating both from wind turbines within the farm and from farms several kilometers upstream. The most common way to include wind farm effects in numerical weather prediction (NWP) models is through a so-called explicit wind farm parameterization (WFP), of which many have been developed in recent years (Fischereit et al., 2022). Today, most widely used models such as WRF or HARMONIE have at least 1 WFP implemented in a research branch of their code (van Stratum et al., 2022). Although NWP models, and their associated implemented WFP variants, share common principles, details on the implementation and features of the codes can profoundly impact model outputs and accuracy. As a result, a comparison on forecast skill between different NWP models and WFP implementations is often warranted, especially for novel implementations.

This deliverable focuses on the efforts within BeFORECAST to implement and test novel WFP implementations in WRF and ALARO (T4.2) and perform a model intercomparison for both annual forecast skill as well as specific extreme events (T4.4). More specifically, the Fitch WFP (Fitch et al., 2012) was implemented and tested in a research branch of the operational RMI ALARO model. The forecast skill of ALARO, both with and without the Fitch WFP, is compared to the Fitch implementation in WRF for the year 2022 as well as for a specific week in February 2022 with high-impact storm events over the Belgian North Sea. Furthermore, a comparison between the long-standing Fitch implementation in WRF and a novel subgrid layout-aware WFP (Ma et al., 2022) is performed. The focus of the current deliverable is on wind speed forecast skill with respect to reference lidar observations within a Belgian offshore wind farm. Wind power forecast accuracy is further discussed in Deliverable D5.3 (Performance assessment of wind farm power- and nowcasting).

The remainder of this deliverable is organized as follows: Section 2 introduces the mesoscale models used in this study, WRF and ALARO, and summarizes their main characteristics. Section 3 describes the wind farm parameterizations implemented in these models, focusing on the widely used Fitch scheme and the novel Ma & Archer approach. Section 4 presents the BeFORECAST mesoscale simulation datasets, including details on model configurations, domains, and time periods. Section 5 provides an intercomparison of the datasets, analyzing forecast skill for wind speed under different configurations and evaluating the impact of activating wind farm parameterizations. Section 6 concludes the report by summarizing key findings and outlining implications for future work.

2 Mesoscale models

2.1 WRF (VKI)

The Weather Research and Forecasting (WRF) model is a mesoscale numerical weather prediction system designed for research and operational purposes (Skamarock et al., 2019). Developed by the National Center for Atmospheric Research (NCAR), the WRF model is supported by a large user community that includes meteorological agencies, research laboratories, universities, and private companies.

WRF solves the fully compressible, nonhydrostatic Euler equations in conservative flux form. Its computational framework is based on a system of nested structured grids, which allows users to refine the resolution of regions of interest while ensuring smooth transitions between domains. The model

employs terrain-following, pressure-based coordinates vertically, with grid spacing that varies as a function of height to better capture atmospheric processes near the surface and aloft.

To represent atmospheric processes, WRF offers a wide range of physics options that can be selected and combined depending on the application. These include parameterizations for microphysics, radiation, planetary boundary layer processes, land-surface interactions, and cumulus convection. This flexibility enables WRF to be applied across scales, from idealized studies to operational weather forecasting and climate research.

2.2 ALARO (RMI)

The Royal Meteorological Institute of Belgium (RMI) utilizes the ALARO numerical weather model, at both 4 km and 1.3 km horizontal resolution, for its operational weather forecasts.

ALARO is a limited-area model developed within the ACCORD consortium and shares its dynamical core with the IFS/ARPEGE global model but differs in its physical parameterizations and in the way the coupling between dynamics and physics is implemented. The boundary layer in ALARO is represented using the TOUCANS turbulence scheme, while microphysical processes follow the approach described by Lopez (2002). Unlike HARMONIE-AROME, ALARO includes an explicit deep-convection scheme (3MT), which allows it to operate across a wide range of horizontal resolutions, from several hundred meters to ten kilometers.

Another key characteristic of ALARO is that it handles physical tendencies in a flux-based framework, integrating changes in prognostic variables such as horizontal wind and turbulent kinetic energy (TKE) over the vertical dimension.

For further details on the physical and dynamical formulation of the ALARO model see Termonia et al. (2018).

Dedicated 15 minute ALARO 4km data at various locations inside the BOZ allows RMI's operational Storm Forecast Tool (Smet et al., 2019), which has been running since 2018, to provide Elia, the Belgian transmission system operator, with probabilistic wind and power forecasts and cut-out alerts.

3 Wind farm parameterizations

Wind turbines interact with the surrounding atmospheric flow during their operation, which influences local weather conditions and energy yield predictions. Due to grid resolution limitations, a mesoscale model cannot explicitly resolve individual turbines; therefore, their influence is accounted for by including a wind farm parameterization (WFP).

Wind turbines extract kinetic energy from the wind, creating an upwind blockage effect and a downwind wake effect. The common underlying aspects of a WFP are a momentum sink term, which accounts for momentum extraction and the resulting wind speed deficit, and a turbulent kinetic energy (TKE) source term, which represents the increase in turbulence generated by the turbines.

Input requirements for a WFP include geometric characteristics of the turbines, such as rotor diameter and hub height; performance specifications, including power and thrust curves as a function of wind speed; and precise turbine locations within the model domain. One limitation of many WFPs is that they

do not explicitly resolve individual wakes; rather, they use a bulk approach to approximate the turbines' overall effect on the atmospheric flow within a grid cell.

Several families of WFPs have been proposed in the literature. The simplest approaches represent turbines as momentum sinks and turbulence sources within the flow (e.g., Fitch et al., 2012). Empirical or analytical wake models approximate wake expansion and velocity deficits using simplified formulas. One of the most common is the Jensen model, which predicts wake growth and wind speed reduction downstream of turbines (Ma et al., 2022).

Hybrid approaches combine physical principles with data-driven methods. For instance, Pan and Archer (2018) use regression on LES results and the geometric properties of wind farms to predict velocity deficits and turbulence.

3.1 Fitch

In the approach of Fitch et al. (2012), wind turbines are treated as a sink of horizontal momentum and a source of turbulent kinetic energy (TKE). More precisely, the effect of the turbines on the horizontal wind vector V = (u, v) and TKE is described by the equations:

$$M\frac{\partial V}{\partial t} = -\frac{1}{2}\rho C_T A_{rotor}|V|V,$$

$$\frac{\partial TKE}{\partial t} = \frac{1}{2}\rho(C_T - C_P)A_{rotor}|V|^3$$

Where ρ is the air density, M the mass of the grid parcel, A_{rotor} the rotor-swept area, and C_t and C_p the thrust and power coefficients. The first equation represents the extraction of momentum from the flow, while the second quantifies the conversion of part of that kinetic energy into turbulence. In numerical models these expressions are discretized both horizontally and vertically: only grid boxes containing turbines receive contributions, and within those boxes only the vertical levels intersecting the rotor disc are affected, with weights proportional to the fraction of A_{rotor} present at that height.

3.1.1 Implementation in ALARO

To represent the wake effects by offshore wind farms, the Royal Meteorological Institute of Belgium (RMI) implemented the wind-farm parameterization of Fitch et al. (2012) in the ALARO model (Van den Bleeken et al. 2025), adapting the earlier HARMONIE-AROME implementation by van Stratum et al. (2022).

The implementation in ALARO differs from that in HARMONIE-AROME in several key aspects. The boundary-layer turbulence is represented by the TOUCANS scheme (Ďurán et al., 2014), which introduces two prognostic turbulence-energy variables. In addition to TKE, the model also predicts the total turbulent energy (TTE), defined as the sum of TKE and turbulent potential energy (TPE). The latter corresponds to the part of potential energy that can be converted into kinetic energy and is proportional to the square of temperature fluctuations (Zilitinkevich et al., 2013). Wind turbines are assumed not to modify TPE, so changes in TTE due to the parameterization are equivalent to changes in TKE; that is, ∂TTE / ∂t = ∂TKE / ∂t, with the right-hand side determined by the second equation above.

A further distinction concerns the way ALARO handles physical tendencies. Rather than integrating temporal tendencies directly, it uses a flux-based formulation. The vertical flux φ_V of horizontal wind velocity is defined as the integral of its tendency over geopotential height z:

$$\varphi_V = -\frac{1}{g}\int_0^{z_{top}} \frac{\partial V}{\partial t} dz$$

where z_{top} denotes the top of the model domain and g is the gravitational acceleration. In practice, the turbine-induced momentum tendency obtained from the Fitch scheme is converted into a corresponding flux according to this relation and then added to the flux contributions from other physical parameterizations. During the model-integration step, these fluxes are used to update the prognostic variables.

Simulations were performed over a European domain that encompasses the Belgian Offshore Wind Energy Zone and neighboring Dutch wind farms. The turbine positions and characteristics were taken from a static database representing the situation at the end of 2022. Comparative runs with the parameterization switched on and off clearly demonstrated the formation of wake effects, with significant downstream wind-speed deficits in the BOZ. These results confirm that the parameterization behaves as expected and that incorporating the Fitch WFP into ALARO enhances the model's capability to reproduce mesoscale wake interactions and improve offshore wind-speed forecasts.

3.2 Ma & Archer

The Ma & Archer WFP (Ma et al. 2022) is a recent approach designed to improve the representation of wind turbine wakes in mesoscale models. The main limitation of the Fitch scheme is that it does not explicitly account for individual wakes and sub-grid wake losses. All the wind turbines in the same cell experience the same wind speed and direction. With typical horizontal grid spacing of 1 to 3 km in operational models today, this can significantly impact simulation accuracy. Ma & Archer address this limitation by incorporating analytical wake models into the parameterization. The approach combines three wake loss models and wake superposition methods in an ensemble to provide a more physically realistic representation of wake effects within the coarse grid of mesoscale models.

The wake loss models used here are the Jensen model, the geometric model, and the Gaussian model; the superposition methods include both superposition of wake deficit (linear and squared) and superposition of the wind speed.

These enhancements enable the scheme to better capture the complexity of subgrid wake interactions, and the uncertainties associated with the engineering models. Consequently, this parameterization is recommended for applications involving coarse resolution, high turbine density, and wind directions aligned with turbine rows, where wake losses are most pronounced.

4 BeFORECAST mesoscale simulation datasets

In this section a summary of the dataset created and used during the project is provided. VKI made available both Reanalysis and Forecast datasets. The difference lies in how the mesoscale model is driven: the former is driven using ERA5, while the latter is driven with the Global Forecasting System. All datasets include results with and without the Fitch scheme. The Reanalysis datasets cover years from 2021 to 2024,

while the forecast are available for period July 2021 to June 2022 and have a 48h lead time. RMI provides forecasts driven by ARPEGE, both with and without WFP. Horizontal grid spacing is 4 km or 1.3 km.

VKI datasets	"Reanalysis"	"Reanalysis"	"Reanalysis"	"Reanalysis"	Forecast
Produced by	VKI	VKI	VKI	VKI	VKI
Time period	2021 – 2024	2023	2023	Jul '21 – Jul '22	Jul '21 – Jun '22
Model	WRF	WRF	WRF	WRF	WRF
IBC & LBC	ERA5	ERA5	ERA5	ERA5	GFS
Resolution	9 – 3 – 1 km	9 – 3 – 1 km	9 – 3 – 1 km	18 – 6 – 2 km	18 – 6 – 2 km
WFP	Fitch ($\alpha = 0.25$)	Fitch ($\alpha = 0$)	Fitch ($\alpha = 1$)	Fitch ($\alpha = 0.25$)	Fitch ($\alpha = 0.25$)
Batch runs	7 + 1 days	7 + 1 days	7 + 1 days	7 + 1 days	2 days + 6 h
Output Data	NEWA for full time period (incl. TKE)	NEWA for full time period (incl. TKE)	NEWA for full time period (incl. TKE)	NEWA for full time period (incl. TKE)	Cf. below
Data time res.	10 min	10 min	10 min	10 min	Hourly + high-freq (every timestep)

RMI datasets	Forecast	Forecast	Forecast	Forecast	Forecast
Produced by	RMI	RMI	RMI	RMI	RMI
Description	ALARO 4 km operational	ALARO 4 km with WFP (experimental)	ALARO 4 km without WFP (experimental)	ALARO 1.3 km with WFP (experimental)	ALARO 1.3 km without WFP (experimental)
Name	ALO4	ALO4_WFP	ALO4_noWFP	ALO1_WFP	ALO1_noWFP
Time period	Jun '21 - May '24	Jun '21 - May '24	Feb 2022	Feb 2022	Feb 2022
Model	ALARO	ALARO	ALARO	ALARO	ALARO
IBC & LBC	ARPEGE	ARPEGE	ARPEGE	ARPEGE	ARPEGE
Resolution	4 km	4 km	4 km	1.3 km	1.3 km
WFP	no	Fitch ($\alpha = 1$)	no	Fitch ($\alpha = 1$)	No
Batch runs	60h	60h	60h	48h	48h
Output Data	10m&100m & turbine hub height WS & WD, T2m, RH2m, 10m gust speed, surfpres, precip, SSRD FDIR (+ model level u,v,q,z,t on tape archive)	10m&100m & turbine hub height WS & WD, T2m, RH2m, 10m gust speed, surfpres, precip, SSRD FDIR (+ model level u,v,q,z,t on tape archive)	50m&100m& 150m&200m & turbine hub height WS & WD (+ surfpres, precip, SSRD FDIR, model level u,v,q,z,t on tape archive)	50m&100m& 150m&200m & turbine hub height WS & WD (+ surfpres, precip, SSRD FDIR, pressure level u,v,q,z,t on tape archive)	50m&100m& 150m&200m & turbine hub height WS & WD (+ surfpres, precip, SSRD FDIR, pressure level u,v,q,z,t on tape archive)
Data time res.	Hourly (+ 15 min BOZ)	Hourly (+ 15 min BOZ)	Hourly	Hourly	Hourly

4.1 VKI datasets

The datasets produced by VKI consist of 2 categories, i.e., an extended reanalysis-driven dataset for an extended time period and a forecast-driven dataset for a time period of 1 year. Subsets of this data can be shared upon reasonable request.

In the remainder of this deliverable, only the forecast dataset is used. The forecast dataset was created using WRF by dynamically downscaling the Global Forecast System (GFS) weather forecast model from the National Centers for Environmental Prediction. The original GFS grid resolution of 28 km was refined to 2 km for an area covering the southern Bight of the North Sea. GFS served as the source for initial and boundary conditions in all WRF simulations.

Characteristics of the dataset:

- Each forecast includes a 6h spin-up followed by a 48h prediction window (forecast for day D: start at D-1 at 18:00 and ends at D+2 at 23:59
- GFS cycle 00 was used to ensure consistency with ALARO simulations.
- Wind farms surrounding the Belgian cluster were included to capture potential inter-farm wake interactions, incorporating farms from the UK and the Netherlands.
- The dataset spans one year, from July 2021 to June 2022.

The numerical setup is:

- Three nested grids for progressively downscaling the global model (see Figure 1): grid resolutions are respectively 18km (D01), 6km (D02, in blue), and 2km (D03, in red)
- The vertical grid consists of 79 non-uniform layers, designed to resolve wind turbine effects on the atmosphere. The model top is approximately 21 km, while output is stored up to 500 m (first 41 eta levels), providing detailed resolution of the atmospheric layers most affected by wind farms (see Figure 2).
- The Fitch wind farm parameterization was activated to represent wake effects, including wind speed deficits downstream of turbines and increased turbulent kinetic energy. The domain includes Belgian and Dutch wind farms as well as neighboring UK farms, as shown in the figure below (Figure 3). Figure 4 shows the wind turbine density in the D03 domain, where we observe a maximum of 19 wind turbines in the same cell. The list of the wind farms included in the simulations is the following:
    - **BE**: Belwind, C-POWER / Thornton (I, II, III), Northwind, Rentel, Mermaid, Northwester 2, Norther, Seastar, Nobelwind
    - **NL**: Egmond aan Zee, Borssele II, Fryslan, Luchterduinen, Prinses Amalia, Borssele I, Borssele III, Borssele IV, Borssele V
    - **UK**: Gunfleet Sands (I, II, III), Scroby Sands, Kentish Flats (+ extension), East Anglia One, Galloper, Greater Gabbard, Thanet, London Array

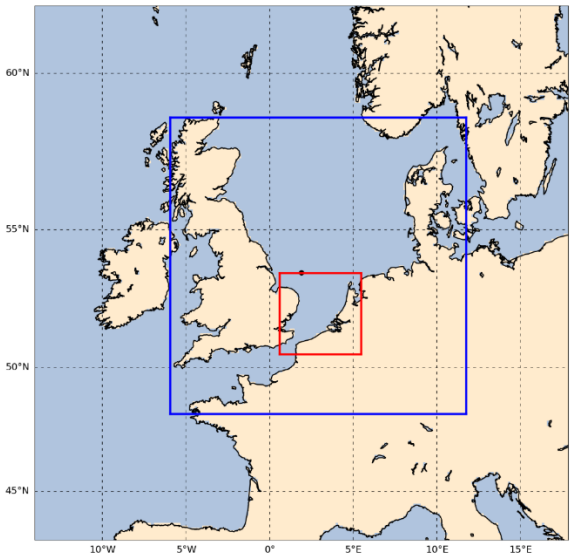

Figure 1 Nested domain configuration used in WRF

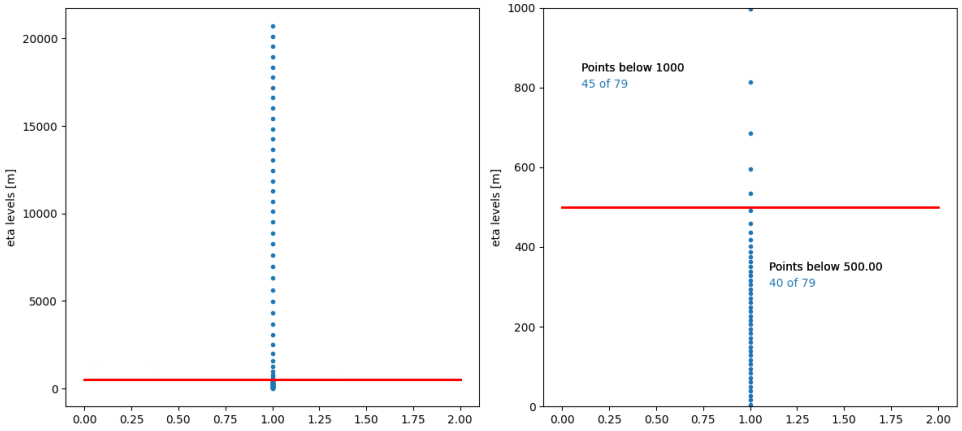

Figure 2 Vertical discretization of the grid

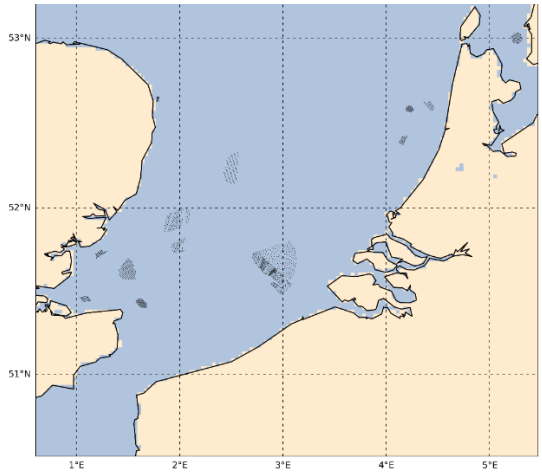

Figure 3 Location of wind turbines included in WRF forecast dataset

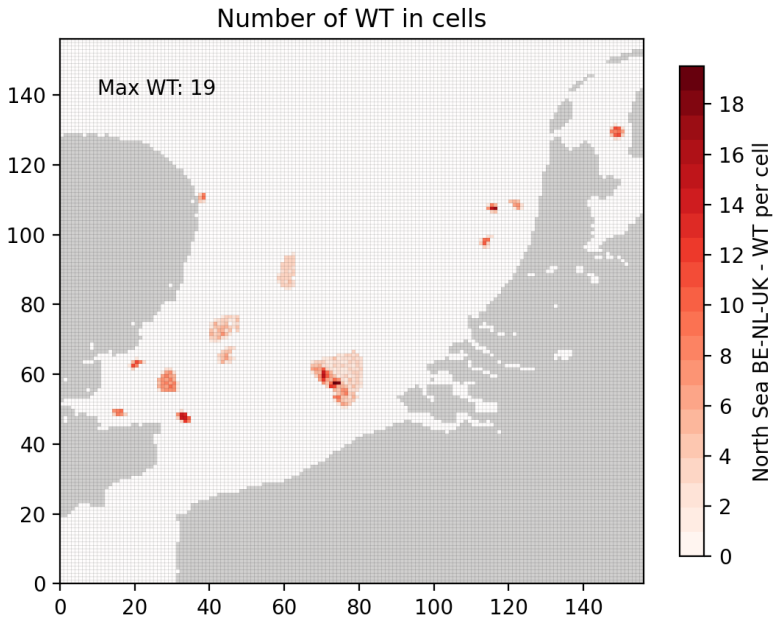

Figure 4 Wind turbine density in the WRF model

Wind turbine power and thrust coefficients were obtained from publicly available sources to ensure transparency and ease of sharing. Turbine locations were extracted from OpenStreetMap[1] and OpenSeaMap[2], while the power curves are generated using the power curve generator available in PyWake[3] ,which requires only public information to generate a realistic power curve (i.e. hub height, rotor diameter, rated power).

To maintain consistency with the global model, GFS boundary conditions were applied hourly, preventing significant drift between WRF and GFS. Model outputs were saved every hour for the innermost domain and up to approximately 500 m in height, covering the atmospheric layers most affected by wind farms.

The output from the model is saved every hour for the innermost domain and up to approximately 500m. The output includes key variables such as:

- Horizontal components of the wind speed at 10m (U10 and V10)
- Velocity field (U, V, W)
- Perturbation temperature T, base state pressure (PB) and perturbation pressure fields (P)
- Turbulent Kinetic Energy field (QKE, which is twice the TKE)
- Cloudiness (CLDFRA)
- Precipitation: RAINC (accumulated total convective precipitation), and RAINNC (accumulated total grid scale precipitation)

[1] https://www.openstreetmap.org/
[2] https://map.openseamap.org/
[3] https://gitlab.windenergy.dtu.dk/TOPFARM/PyWake

Beside the standard WRF output files, the WRF *climate diagnostics* are activated, which output for the surface variables T2, Q2, TSK, U10, V10, 10 m wind speed, RAINCV, RAINNCV the following statistics: maximum and minimum, mean value, and standard deviation of the mean.

In addition to the hourly fields, 13 probes have been added to extract at each time step a time series of variables in specific locations. The locations of the probes are given in the following table and correspond to the positions of 4 Lidars (Westhinder, Lichteiland Goeree, Europlatform, Borssele B) and the positions of the substations for the wind farms on the Belgian cluster.

Table 1 Probe locations in WRF simulations

Name	ID	LAT	LON
Westhinder	WHi	51.389	2.438
Lichteiland Goeree	LEG	51.933	3.667
Europlatform	EPL	51.998	3.275
Borssele B	BSB	51.726	2.966
Seastar	Seast	51.624	2.844
Mermaid	Merma	51.712	2.724
Rentel	Rente	51.576	2.919
Norther	North	51.514	2.991
Northwester 2	Nrtwe	51.688	2.759
Belwind I	Belwi	51.695	2.817
Nobelwind	Nobel	51.690	2.825
Northwind	Nrtwi	51.620	2.918
Thornton	Thor	51.533	2.955

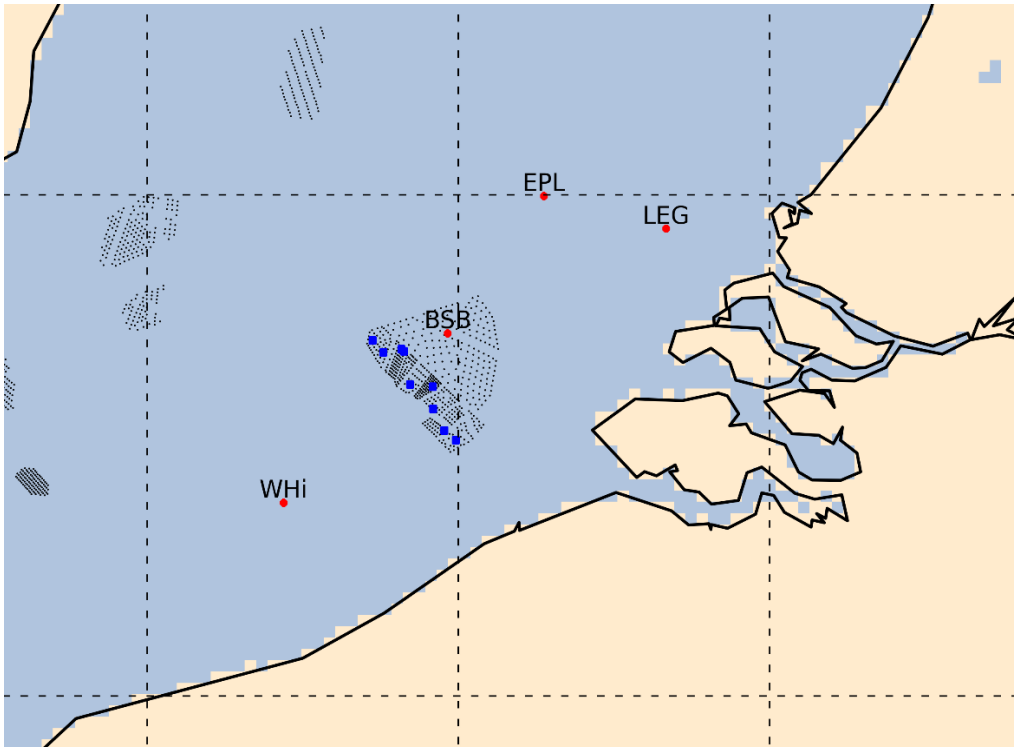

The variables included in the probes are:

- Vertical profiles of U, V, W, potential temperature TH, geopotential height PH, water vapor mixing ration QV and pressure PR
- Values for 2m temperature (t) and vapor mixing ratio (q), surface pressure (psfc), skin temperature (tsk), rainfall (rainc, rainnc), ...
- Wind speed and direction at 10m and 100m, temperature, humidity, Turbulent Kinetic Energy, precipitation wind gusts, surface pressure, cloudiness and radiation

5 Intercomparison of datasets

This section presents the comparison between two mesoscale models, ALARO and WRF, focusing on their ability to predict wind speed when compared to lidar observations. The objective is to evaluate how these models perform under different configurations, including cases with and without wind farm parameterization (WFP), and to understand the impact of model setup choices on forecast accuracy.

To carry out this comparison, wind speed was sampled at specific reference locations for each wind farm. Two approaches were considered for defining these locations: (1) the average position of all turbines within the wind farm, and (2) operational locations used in ALARO, ensuring consistency with previous analyses conducted at RMI.

The comparison between the models and the measurementsare carried out using the python verification package developed by 3E within this project and described in deliverable D5.1 (verif3E tool).

Figure 5 illustrates the bias (bottom) and MAE (top) of the numerical models compared to Lidar measurements at an anonymous wind farm for the period January to June 2022. Both ALARO and WRF

without WFP show similar performance, with a positive bias around 1.25 m/s and a MAE close to 2.0 m/s. This indicates that, in the absence of WFP, both models tend to overestimate wind speed.

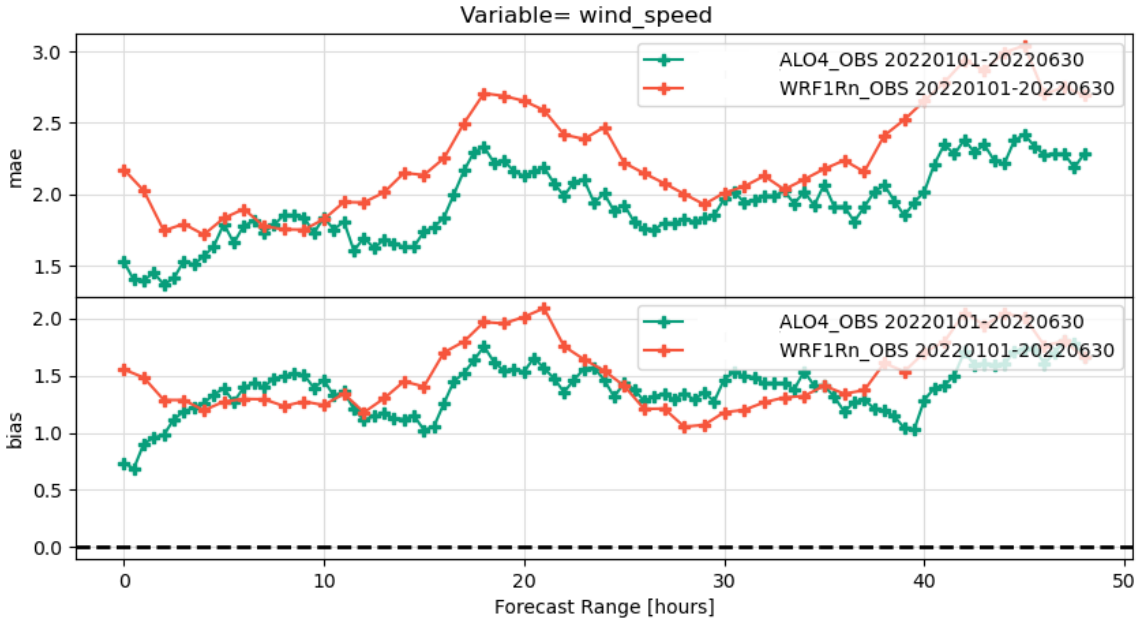

Figure 5 BIAS and MAE from verif3E tool for ALO4 and WRF (no WFP) against lidar observations at an anonymous wind farm.

When WFP is activated (Figure 6), the bias becomes negative, clearly showing that the models now underestimate wind speed relative to Lidar observations. Both ALARO and WRF exhibit similar behavior, with bias oscillating around -0.25 m/s. Interestingly, the MAE decreases from approximately 2.0 m/s without WFP to about 1.4 m/s with WFP enabled, suggesting that the inclusion of wind farm effects improves overall accuracy despite introducing a slight negative bias due to overestimation of wakes.

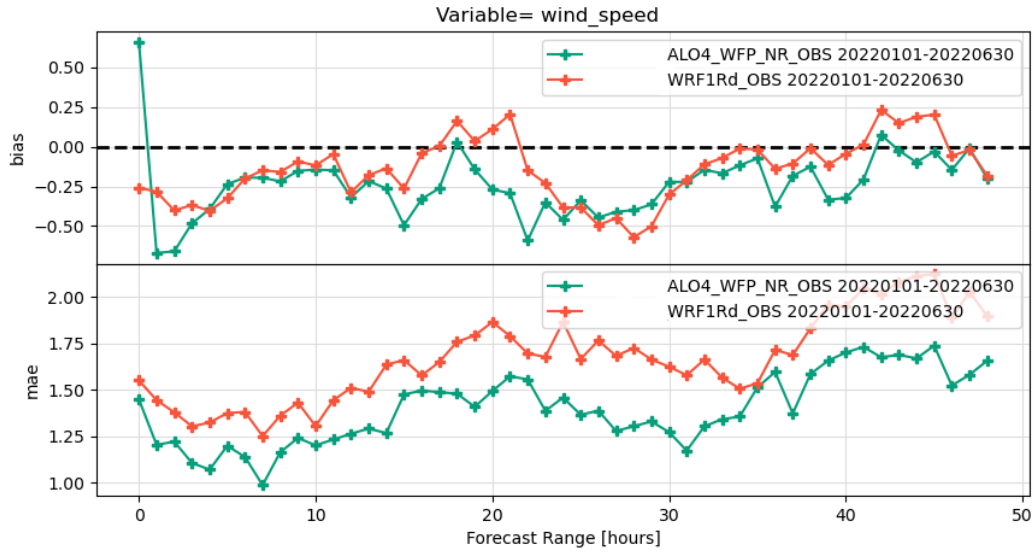

Figure 6 BIAS and MAE from verif3E tool for ALO4_WFP and WRF at RMI locations, against lidar observations at anonymous wind farm.

Figure 7 explores the sensitivity of bias (left), MAE (center), and NSTD (right) to the choice of reference location for wind speed sampling in both models.
More in detail:

- ALO4_WFP uses the same "operational" locations as in ALO4. These locations are confidential and will not be disclosed.
- ALO4_WFP_NR and WRF1d use "experimental" locations defined by RMI and tested to assess their suitability.
- WRF1c employs different reference locations defined as the average location of the wind turbines for each wind farm and are given in Table 1.

The results indicate that location selection significantly impacts all three metrics, highlighting the importance of carefully defining reference points when characterizing wind farm behavior and validating model performance.

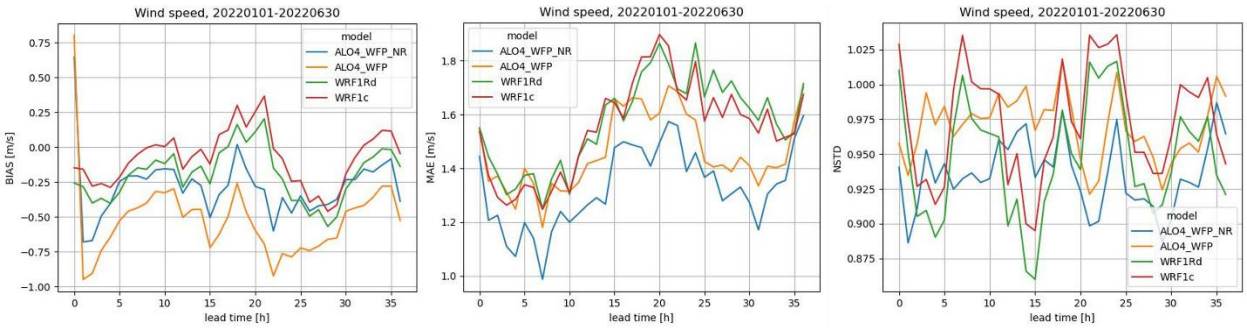

Figure 7 BIAS (left) and MAE (center) and NSTD (left) of ALO4_WFP and WRF against lidar observations at an anonymous wind farm.

Figure 8 shows bias and MAE as a function of wind direction. Models without WFP (ALO4 and WRF1Rn) consistently exhibit a positive bias across all directions. For WRF with WFP (WRF1c and WRF1Rd), the bias varies between positive and negative depending on direction, while ALARO with WFP (ALO1_WFP and ALO4_WFP_NR) generally shows negative or near-zero bias, except for the southwest (SW) direction. Notably, for the SW direction, which is the dominant wind direction and where coastal effects and neighboring farm wakes are minimal, the bias is positive for all models, suggesting that even with WFP, certain directional conditions remain challenging to model accurately. There might also be a shading effect at play here (caused by nearby wind turbines) as the lidar is located inside the wind farm.

For an anonymous wind farm, Figure 9 compares wind speed from both ALARO and WRF against Lidar measurements (blue line) during Storm Eunice on February 18, 2022. All models capture the ramp-up in wind speed, but WRF underestimates the peak, whereas ALARO better reproduces the maximum observed value.

Finally, Figure 10 presents the wind speed deficit caused by the presence of wind farms for three sites: Norther (left), Seastar (center), and Mermaid (right). The plots illustrate how different models (ALARO and WRF) and grid resolutions (ALARO at 1 km and 4 km) influence the predicted deficit (calculated as the average difference between runs of the same model with and without WFP). Overall, WRF at 2 km resolution consistently predicts the largest wind speed deficit, emphasizing the role of resolution and parameterization in wake effect modeling.

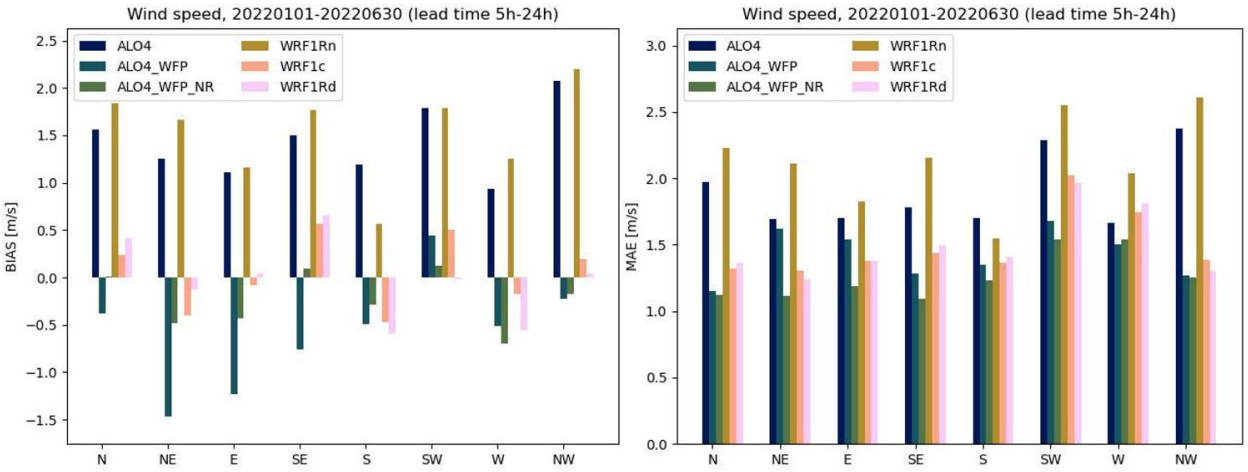

Figure 8 BIAS (left) and MAE (right) of ALO4, ALO4_WFP and WRF (with and without WFP) against lidar observations at an anonymous wind farm, split per wind direction.

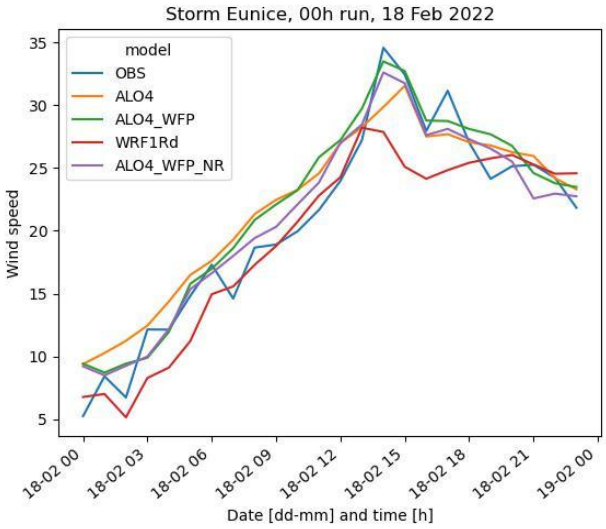

Figure 9 Time series of ALO4, ALO4_WFP, ALO4_WFP_NR and WRF against lidar observations at an anonymous wind farm, for storm Eunice on 18 February 2022.

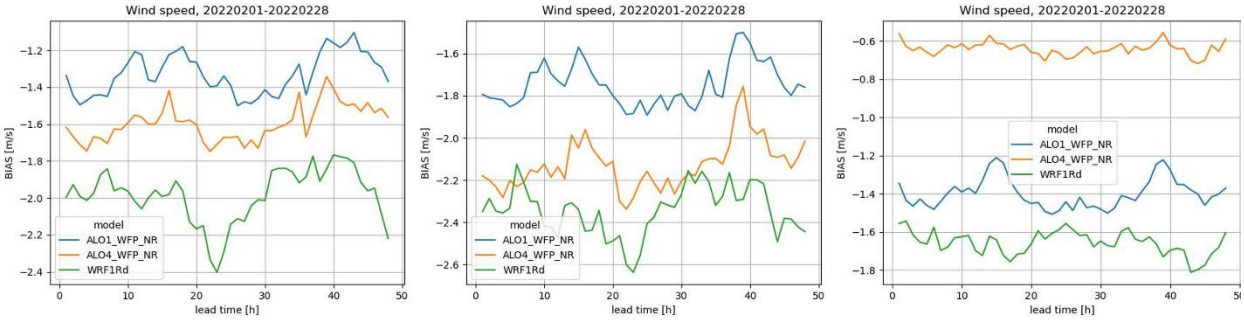

Figure 10 Wind farm effects (wind speed deficit) for ALO1, ALO4 and WRF at Norther (left), Seastar (center), and Mermaid (right) wind farms.

6 Conclusion

This deliverable evaluated the performance of mesoscale models WRF and ALARO in predicting wind speed for offshore wind farms, with and without wind farm parameterization (WFP). The analysis covered long-term verification for the first half of 2022 and a detailed case study of Storm Eunice in February 2022. Comparisons were made against lidar observations using bias, mean absolute error (MAE), and normalized standard deviation (NSTD) metrics.

The results clearly demonstrate the benefit of activating WFP in mesoscale models. Without WFP, both ALARO and WRF exhibit a positive bias of approximately **+1.25 m/s** and a MAE near **2.0 m/s**, indicating systematic overestimation of wind speed due to neglecting wake effects. When WFP is enabled, the bias shifts to around **-0.25 m/s**, and MAE decreases to **1.4 m/s**, representing a substantial improvement in accuracy. These improvements are consistent across both models, with similar performance when WFP is active. Directional analysis shows that WFP reduces bias for most wind directions, although some residual positive bias remains for the dominant southwest flow, where coastal and inter-farm effects are minimal. High-resolution simulations confirm that WRF at 2 km resolution predicts the largest wake-induced deficits, while increasing ALARO's resolution from 4 km to 1 km yields limited additional benefit.

Overall, the inclusion of WFP significantly enhances forecast skill by reducing systematic overprediction and improving representation of wake effects. These findings underline the importance of wake-aware modeling for reliable offshore wind resource assessment and operational forecasting.

7 Dissemination

The work performed by RMI was disseminated in the following forms:

Conference presentation: Smet, G., Van den Bleeken, D., Van den Bergh, J., Dehmous, I., Degrauwe, D., Van Ginderachter, M., and Deckmyn, A. (2024): Improving wind power forecasts in the Belgian North Sea, EMS Annual Meeting 2024, Barcelona, Spain, 1–6 Sep 2024, **https://doi.org/10.5194/ems2024-872**.

Journal publication: Van den Bleeken, D., Smet, G., Van den Bergh, J., Dehmous, I., Degrauwe, D., Van Ginderachter, M., and Deckmyn, A. (2025). Improving wind power forecasts in the Belgian North Sea with a wind farm parameterization and a neural network. *Adv. Sci. Res., 22*, 59–67. **https://doi.org/10.5194/asr-22-59-2025**

8 References

Ďurán, I. B., Geleyn, J.-F., and Váňa, F. (2014). A compact model for the stability dependency of TKE production–destruction–conversion terms valid for the whole range of Richardson numbers. *Journal of the Atmospheric Sciences, 71*, 3004–3026. **https://doi.org/10.1175/JAS-D-13-0203.1**

Ďurán, I. B., Geleyn, J.-F., Váňa, F., Schmidli, J., and Brožková, R. (2018). A Turbulence Scheme with Two Prognostic Turbulence Energies. *Journal of the Atmospheric Sciences, 75*, 3381–3402. **https://doi.org/10.1175/JAS-D-17-0310.1**

Fischereit, J., Brown, R., Larsén, X.G., Badger, J. and Hawkes, G., 2022. Review of mesoscale wind-farm parametrizations and their applications. *Boundary-Layer Meteorology*, *182*(2), pp.175-224. **https://doi.org/10.1007/s10546-021-00652-y**

Fitch, A. C., Olson, J. B., Lundquist, J. K., Dudhia, J., Gupta, A. K., Michalakes, J., and Barstad, I. (2012). Local and mesoscale impacts of wind farms as parameterized in a mesoscale NWP model. *Monthly Weather Review, 140*, 3017–3038. https://doi.org/10.1175/MWR-D-11-00352.1

Lopez, P. (2002). Implementation and validation of a new prognostic large-scale cloud and precipitation scheme for climate and data-assimilation purposes. *Quarterly Journal of the Royal Meteorological Society, 128*, 229–257. https://doi.org/10.1256/00359000260498879

Ma, Y., Archer, C.L., and Vasel-Be-Hagh, A. (2022). Comparison of Individual versus Ensemble Wind Farm Parameterizations Inclusive of Sub-grid Wakes for the WRF Model. *Wind Energy, 25*(9), 1573–1595. https://doi.org/10.1002/we.2758

Skamarock, C., Bogumiła Klemp, Jimy Dudhia, O. Gill, Zhiquan Liu, Judith Berner, Wei Wang, G. Powers, Greg Duda, Dale Melvyn Barker and Xiangyu Huang. (2019). A Description of the Advanced Research WRF Model Version 4. *(NCAR Technical Note, NCAR/TN-556+STR, 145 pp.)*

Smet, G., J. Van den Bergh, and P. Termonia. (2019). Probabilistic storm forecasts for wind farms in the North Sea. *ALADIN–HIRLAM Newsletter, 12*, 17–24.

Termonia, P., Fischer, C., Bazile, E., Bouyssel, F., Brožková, R., Bénard, P., Bochenek, B., Degrauwe, D., Derková, M., El Khatib, R., Hamdi, R., Mašek, J., Pottier, P., Pristov, N., Seity, Y., Smolíková, P., Španiel, O., Tudor, M., Wang, Y., Wittmann, C., and Joly, A. (2018). The ALADIN System and its canonical model configurations AROME CY41T1 and ALARO CY40T1. *Geoscientific Model Development, 11*, 257–281. https://doi.org/10.5194/gmd-11-257-2018

van Stratum, B., Theeuwes, N., Barkmeijer, J., van Ulft, B., and Wijnant, I. (2022). A one-year-long evaluation of a wind-farm parameterization in HARMONIE-AROME. *Journal of Advances in Modeling Earth Systems, 14*, e2021MS002947. https://doi.org/10.1029/2021MS002947

Van den Bleeken, D., Smet, G., Van den Bergh, J., Dehmous, I., Degrauwe, D., Van Ginderachter, M., and Deckmyn, A. (2025). Improving wind power forecasts in the Belgian North Sea with a wind farm parameterization and a neural network. *Adv. Sci. Res., 22*, 59–67. https://doi.org/10.5194/asr-22-59-2025

Zilitinkevich, S., Elperin, T., Kleeorin, N., Rogachevskii, I., and Esau, I. (2013). A hierarchy of energy- and flux-budget (EFB) turbulence closure models for stably-stratified geophysical flows. *Boundary-Layer Meteorology, 146*, 341–373. https://doi.org/10.1007/s10546-012-9768-8